Electronic Interaction between Nitrogen-Doped Graphene and Porphyrin Molecules

Van Dong Pham,[†] Jérôme Lagoute,[*,†] Ouafi Mouhoub,[†] Frédéric Joucken,[‡] Vincent Repain,[†] Cyril Chacon,[†] Amandine Bellec,[†] Yann Girard,[†] and Sylvie Rousset[†]

[†]Laboratoire Matériaux et Phénomènes Quantiques, CNRS-Université Paris 7, 10 Rue Alice Domon et Léonie Duquet, 75205 Paris Cedex 13, France and
[‡]Research Center in Physics of Matter and Radiation (PMR), University of Namur, 61 Rue de Bruxelles, 5000 Namur, Belgium

ABSTRACT The chemical doping of graphene is a promising route to improve the performances of graphene-based devices through enhanced chemical reactivity, catalytic activity, or transport characteristics. Understanding the interaction of molecules with doped graphene at the atomic scale is therefore a leading challenge to be overcome for the development of graphene-based electronics and sensors. Here, we use scanning tunneling microscopy and spectroscopy to study the electronic interaction of pristine and nitrogen-doped graphene with self-assembled tetraphenylporphyrin molecules. We provide an extensive measurement of the electronic structure of single porphyrins on Au(111), thus revealing an electronic decoupling effect of the porphyrins adsorbed on graphene. A tip-induced switching of the inner hydrogen atoms of porphyrins, first identified on Au(111), is observed on graphene, allowing the identification of the molecular conformation of porphyrins in the self-assembled molecular layer. On nitrogen-doped graphene, a local modification of the charge transfer around the nitrogen sites is evidenced *via* a downshift of the energies of the molecular elecronic states. These data show how the presence of nitrogen atoms in the graphene network modifies the electronic interaction of organic molecules with graphene. These results provide a basic understanding for the exploitation of doped graphene in molecular sensors or nanoelectronics.

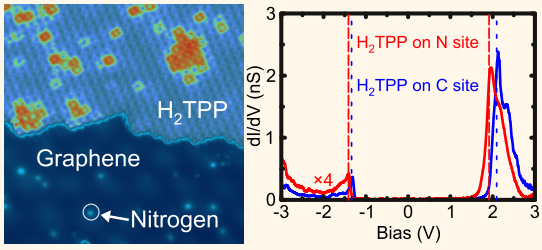

KEYWORDS: graphene · nitrogen doping · tetraphenylporphyrins · scanning tunneling microscopy · scanning tunneling spectroscopy · charge transfer · self-assembly

Graphene is a two-dimensional carbon material with unique physical and chemical properties[1,2] that make it an enticing material for a broad range of technological applications including novel electronics,[3−5] gas sensing,[6−8] and catalysis.[9−11] In this context, controlling the properties of graphene and mastering its interaction with other species are cornerstones for the realization of graphene-based devices. Among the methods explored to tune the properties of graphene, the substitutional chemical doping appears as a promising route.[12] The use of nitrogen doped (N-doped) graphene can improve electrochemical reactions for biosensing applications[13] or provide an efficient catalyst for oxygen reduction.[14] Theoretical studies have shown that the spatial variation of the electron density around nitrogen sites can explain the chemical reactivity of N-doped graphene.[15] Therefore, understanding the atomic-scale interaction between a molecule and a doped graphene sheet will help to improve the future rational designing of graphene-based devices. However, experimental data are still lacking, and only little is known on the local interaction between molecules and graphene doping sites.

Here, we present an extensive low-temperature scanning tunneling microscopy/spectroscopy (STM/STS) study of the electronic properties of 5,10,15,20-tetraphenyl-21*H*,23*H*-porphyrin molecules (H_2TPP) adsorbed on pristine and N-doped graphene on SiC(000$\bar{1}$). Porphyrins have been widely investigated for the functionalization of carbon materials. Many studies have been performed on porphyrin−nanotube composites,[16] and it was shown that H_2TPPs lead to an efficient energy transfer under light excitation.[17] The functionalization of graphene with different types of porphyrins

* Address correspondence to jerome.lagoute@univ-paris-diderot.fr.

Received for review June 26, 2014 and accepted September 4, 2014.

Published online September 04, 2014
10.1021/nn503753e

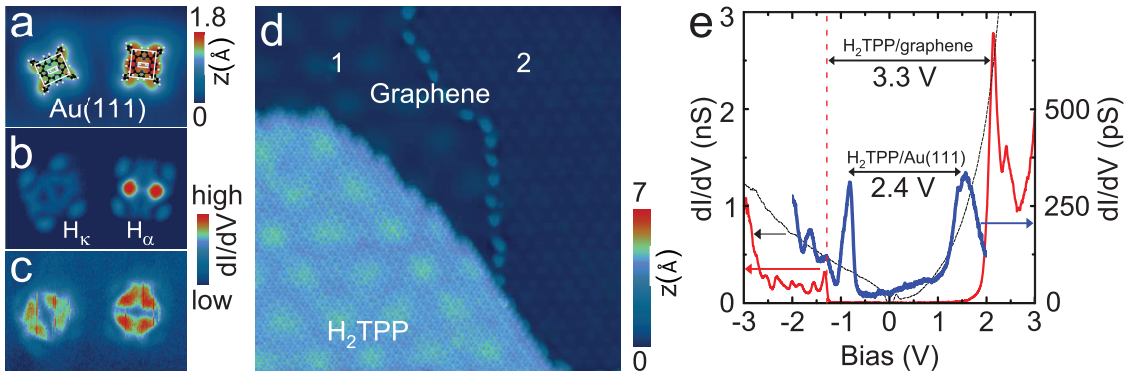

Figure 1. (a) Topography (4 × 6 nm^2, −0.8 V, 40 pA) of two H_2TPP molecules on a Au(111) substrate. The large rectangles are a guide to the eye joining the top C−C bonds of the phenyl groups. The small rectangles indicate the inner hydrogen pairs. (b) Conductance map of the HOMO state of the two molecules at −0.8 V. (c) Conductance map of the LUMO state of the two molecules at +1.5 V (in images a−c the scan direction is vertical). (d) Large-scale image (100 × 100 nm^2, +2 V, 100 pA) of self-assembled H_2TPP on pristine graphene. (e) Representative d*I*/d*V* spectra measured on a pristine graphene area (black dashed curve) and over the center of H_2TPP on Au(111) (blue curve) and H_2TPP on undoped graphene (red curve).

has been used to realize sensitive electrochemical detection of molecules,[18,19] for optical limiters,[20] or to improve the conductivity of graphene films.[21] Here, we use free-base porphyrins as prototype molecules for the study of molecule/doped-graphene interactions. On pristine graphene, at room temperature, the molecules form a two-dimensional square-like lattice with a molecule−substrate electronic coupling reduced as compared to a metallic surface. High-resolution STM images reveal the positions of the inner hydrogen atoms and the random switching between the two tautomer forms, allowing a precise identification of the structures of the molecules on graphene. On N-doped graphene, imaging and local spectroscopy of H_2TPP reveal that the molecules located around a nitrogen site undergo a downshift of their highest occupied molecular orbital (HOMO) and lowest unoccupied molecular orbital (LUMO) states. This indicates that the electronic interaction of the molecules with graphene is different at nitrogen sites than at carbon sites. We show that this effect is not spatially limited to the nitrogen atomic site but spreads over almost 1 nm around the nitrogen atoms.

RESULTS AND DISCUSSION

We have first studied H_2TPP on a Au(111) substrate as a reference. Figure 1a shows the topography of two individual H_2TPP molecules recorded at −0.8 V. It has been shown that the adsorption of H_2TPP on a metallic substrate induces a conformational change of the molecule leading to a rotation of the phenyl groups that are no longer contained in the plane of the macrocycle. As a consequence, the molecule has a rectangular shape. This leads to two inequivalent positions of the central hydrogen pair, which can be parallel (H_κ configuration) or perpendicular (H_α configuration) to the long side of the rectangle joining the top C−C bonds of the phenyl groups (see molecular model in Figure 1a).[22]

In the H_α configuration (Figure 1a, right), two bright lobes appear around the hydrogen positions. In the H_κ configuration (Figure 1a, left) the lobes are no longer observed. The d*I*/d*V* spectrum, which corresponds to the local density of states (LDOS), measured above the molecule in the H_α configuration (see Figure 1e, blue curve) reveals the energy position of the HOMO and LUMO states at −0.83 ± 0.05 and +1.55 ± 0.07 V, respectively, corresponding to an electronic gap of 2.4 eV (in the paper, the error estimation corresponds to the standard deviation of a series of measurements). It is worth noting that the experimental measurement of the HOMO−LUMO gap of H_2TPP is very scarce in the literature. Photoemission experiments on 8 monolayers of H_2TPP/Au(111) have given a gap value of 2.9 eV, which is close to our measurement.[23] STM break junction experiments with gold electrodes have given a gap value of 2.7 eV for different types of porphyrin molecules.[24] However, in the specific case of H_2TPP, this technique failed to give a measurement of the HOMO−LUMO gap. The conductance map of the HOMO state (Figure 1b), which corresponds to the LDOS map, clearly reflects the difference between the two configurations H_α and H_κ that exhibit a 2-fold symmetry. The LUMO state, however, reveals a 4-fold symmetry of the wave function (Figure 1c). The vertical noise observed in Figure 1c corresponds to the random switching of hydrogen atoms between H_α and H_κ configurations,[22,25] which could not be avoided at this bias voltage. On the contrary, at the voltage of the HOMO state (−0.8 V), the two configurations are more stable, allowing imaging without switching and the possibility to induce a controlled switching with the STM tip (see Supporting Information Figure S1).

On graphene, the behavior of porphyrins under adsorption is different. We could not measure single molecules as they were swept by the STM tip during scanning, which is indicative of a weaker molecule−substrate interaction on graphene than on Au(111).

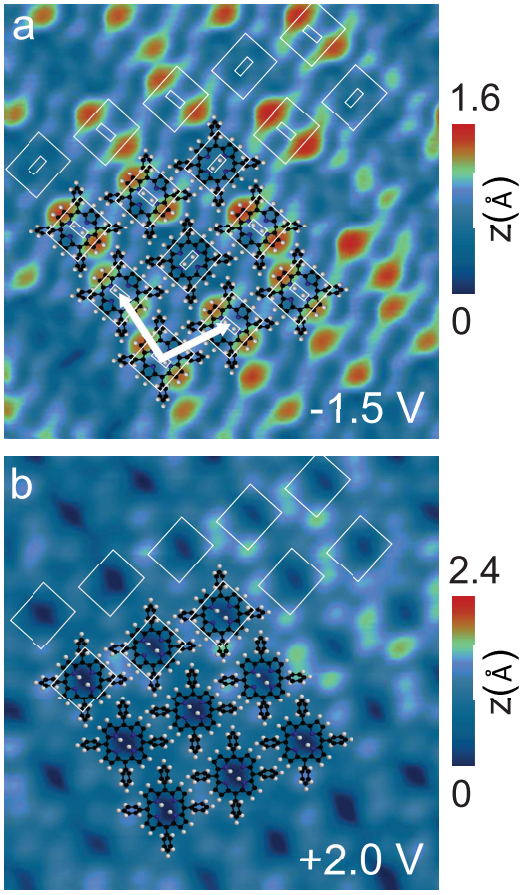

Figure 2. High-resolution STM images (8 × 8 nm^2) of a H_2TPP array on pristine graphene, recorded at (a) −1.5 V, 20 pA and (b) +2 V, 20 pA energies. The molecular models show the structure of the molecular lattice and mark the tautomer forms corresponding to the bright and dark molecules in (a). In (b) the images do not allow the identification of the position of the inner hydrogen atoms; therefore, only one tautomer form is used in the model. The white rectangles are a guide to the eye for the H_α and H_κ configurations (see Figure 1a).

After room-temperature annealing, the molecules self-assemble and form highly ordered stable structures. Figure 1d shows an area of the sample partly covered by a molecular array (left bottom part). Two graphene domains (marked 1 and 2 in Figure 1d) separated by a grain boundary can be seen exhibiting two different moiré patterns due to the misorientation angle between the two top graphene layers. The moiré pattern of domain 1 is clearly seen through the molecular layer, indicating that the molecular island is adsorbed on domain 1. Furthermore, the edge at the bottom right part of the island runs along the limit of domain 2, indicating that the molecule island is partly bounded by the grain boundary that naturally limits the coherency of the 2D self-organized growth (see also Figure S2). In order to understand the orientation and the molecular conformation within the H_2TPP layer, we recorded molecular resolution images. Figure 2 shows small-scale STM images (8 × 8 nm^2) of a H_2TPP array at bias voltages close to HOMO and LUMO energies (Figure 2a and b, respectively). The molecules self-organize into near-square lattice structures with a lattice constant of $a = 1.41 \pm 0.01$ nm and an angle of 96.8°. The symmetry of the molecular lattice is not compatible with that of graphene, indicating that the molecule−molecule interaction is larger than the molecule−substrate interaction as previously reported in theoretical calculations[26] and experimental observation of H_2TPP on highly oriented pyrolytic graphite.[27] Similar to the observation on Au(111) reported in Figure 1b, at the HOMO energy, the molecules appear either with or without two bright lobes corresponding to the H_α and H_κ configurations, respectively (Figure 2a). A series of successive topographical images reveal a random switching over time between the two configurations, as shown in supplementary video 1. This is an intersting fact, as it reveals that the current induced hydrogen switch previously reported on Ag(111)[22] can be generalized to a variety of other substrates such as Au(111) and graphene, which exhibit very different surface reactivity and electronic properties. At the LUMO energy (Figure 2b), the STM images display four lobes centered around the phenyl groups that are again consistent with the molecular orbitals observed on Au(111) (Figure 1c). The local electronic structure of porphyrins on graphene was investigated by d*I*/d*V* spectroscopy. On the uncovered pristine graphene area, the spectrum exhibits a central gap feature around the Fermi level delimited by two onsets corresponding to the inelastic excitation of an acoustic phonon[28] (see Figure 1e, black dashed curve). It has been pointed out that this central gap feature is not observed by all the groups and may depend on the particular tip−sample geometry[29] and on the substrate.[30] In our case, we systematically observed it when using calibrated tips previously checked on a Au(111) surface until the Shockley state feature could be clearly observed in the spectroscopy. It is worth noticing that there is no measurable change within our experimental precision of the spectrum on the pristine graphene before and after adsorption of H_2TPP molecules. The spectrum measured above the H_2TPP molecules shows the HOMO and LUMO resonances respectively at -1.34 ± 0.04 and $+2.00 \pm 0.07$ V, yielding an apparent gap of 3.3 eV. The value of the gap is much larger than that measured on Au(111) (2.4 eV), indicating an electronic decoupling of H_2TPP on graphene similarly to the effect reported for C_{60} molecules.[31] The decoupling is further confirmed by the full widths at half-maximum (fwhm) of the resonances that are measured at 0.06 ± 0.02 V for the HOMO and 0.15 ± 0.02 V for the LUMO on graphene, which are smaller than the values measured on Au(111) (0.16 ± 0.03 and 0.43 ± 0.05 V for the HOMO and LUMO, respectively). The decoupling measured in the electronic spectra is consistent with the weak

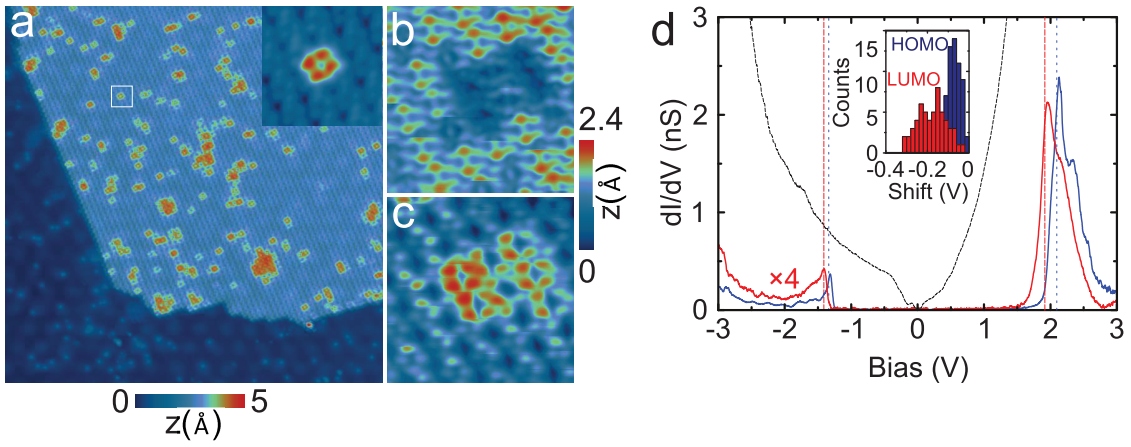

Figure 3. (a) Large-scale image (100 × 100 nm^2, +2 V, 50 pA) of an island of self-assembled H_2TPP molecules on nitrogen-doped graphene. The inset is a zoomed image (6 × 6 nm^2) corresponding to the area marked by the white square (using the same color scale as b and c). (b, c) Zoomed-in images (8 × 8 nm^2) of molecules around a N-doped site at −1.5 V (b) and +2 V (c) (current set point 40 pA). (d) Typical d*I*/d*V* spectra recorded on carbon area of N-doped graphene (dashed black) and comparative d*I*/d*V* spectra of H_2TPP molecules on carbon (blue) and nitrogen (red) sites. The vertical dashed lines mark the energy position of the measured mean values of HOMO and LUMO states on carbon (blue) and nitrogen (red) sites. The inset is the distribution of the energy shifts of the HOMO and LUMO states measured on the molecular island.

interaction with graphene deduced from the diffusion of individual molecules during STM imaging and with the structure of the molecular array.

We now turn to the interaction of the molecules with N-doped graphene. STM/STS have been used to study the atomic and electronic structure of N-doped graphene.[32−34] STS measurements have shown that the insertion of nitrogen atoms in the carbon lattice induces a localized unoccupied state confirmed by calculations[33,35] as well as a charge redistribution extending over several carbon sites surrounding the nitrogen atoms. Figure 3a shows a submonolayer of self-assembled porphyrins on N-doped graphene after deposition at 4.6 K followed by RT annealing. Interestingly, the hydrogen switching is also observed in this area even for molecules at the nitrogen sites (supplementary video 2). On the bare graphene areas, point defects are observed corresponding to nitrogen atoms inserted in the carbon lattice[33] with a doping density of 0.08%. It is worth noticing that we did not observe the molecules in these areas, indicating that the nitrogen sites do not trap the molecules during surface diffusion at room temperature. In the molecular array, a small fraction of the molecules appears higher at +2 V. As shown in Figure 3b and c recorded respectively at −1.5 and +2 V, this tremendous topographic change is due to an electronic effect. Indeed, the molecules that appear higher in Figure 3c appear slightly lower in Figure 3b (by about 1 Å in both cases). For bias voltages inside the gap between the HOMO and LUMO, all the molecules in this area appear identical (see Supporting Information Figure S3).

This bias-dependent contrast can be explained by d*I*/d*V* measurements on the molecular layer. First, as a reference, we have measured the spectrum on uncovered parts of N-doped graphene, which shows the phonon feature around the Fermi level together with a minimum at −0.1 V corresponding to the Dirac point that is typical of the electronic local density of states of N-doped graphene.[32,33] For the molecules out of doping sites, the representative spectrum shown in Figure 3d (blue curve) presents resonances at −1.34 ± 0.02 and +2.10 ± 0.03 V, leading to a gap of 3.4 eV, similar to the case of undoped graphene. The spectra on bright molecules (Figure 3d, red curve) exhibit HOMO and LUMO resonances at −1.41 ± 0.02 and +1.92 ± 0.07 V, respectively, leading to a gap of 3.3 eV. We measured the energy shifts $E^N - E^C$ where E^N is the energy of the HOMO (LUMO) peak on a H_2TPP molecule on a nitrogen site and E^C is the energy of the HOMO (LUMO) peak on a H_2TPP molecule on a carbon site. The distribution of the shift values is displayed in the inset of Figure 3d. The ensemble average values of the energy shifts are −0.07 ± 0.03 V for the HOMO and −0.18 ± 0.07 V for the LUMO. Moreover, series of measurements of the peak positions on several molecular islands confirm the observed energy shift (see Supporting Information Figure S4). This explains the voltage-dependent contrast reported in Figure 3b,c. At +2 V, only the LUMO state of the molecules on N sites is integrated in the tunneling current, leading to an increased conductance. As a consequence, to keep a constant tunneling current, the tip must be retracted further above these molecules, leading to an increased apparent height. At −1.5 V, however, the HOMO state is totally integrated only for the other molecules, while for the molecules above the N sites, the bias is at the edge of the HOMO state. Therefore, the tip must be further approached toward the molecules at doping sites in order to maintain the current set point, leading to a reduced apparent height for the molecules above the nitrogen sites. This also explains the lower intensity

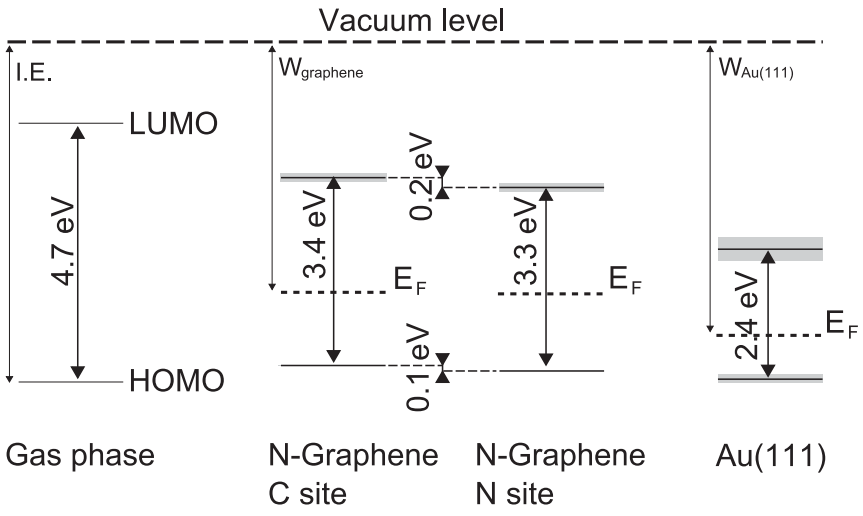

Figure 4. Schematic drawing showing the shift and broadening of the HOMO and LUMO states of H_2TPP molecules from the gas phase (using *ab initio* data from ref 36) to adsorption on N-doped graphene and Au(111) substrate. The energy levels are positioned with respect to the vacuum level using the calculated ionization energy (I.E.)[36] for the gas phase, and the work functions $W_{graphene}$ = 4.6 eV for graphene and $W_{Au(111)}$ = 5.3 eV for Au(111).

of the d*I*/d*V* spectrum at the nitrogen site (Figure 3d). The shift of the HOMO and LUMO states to lower energy indicates a filling of the molecular states, revealing a charge transfer toward the molecules at the nitrogen sites. The slight reduction of the gap of the molecules at these sites further suggests that the electronic interaction between the molecules and the graphene is increased above the nitrogen sites. Therefore, these measurements reveal that the doping sites of N-doped graphene act as electron donors for the porphyrin molecules. We have probed spatial extension of this effect by measuring the ratio between the density of bright molecules at +2 V and the density of nitrogen atoms. We found a ratio of 2.2. Using a geometrical model we found that an interaction radius of 8 Å around the nitrogen atoms reproduces the experimental density ratio as well as the patterns observed for bright molecules (single molecules, clusters, linear chains) (see Supporting Information Figure S5). This radius corresponds to the extension of the main pattern of increased density of states induced by the presence of a nitrogen atom in the carbon lattice[33] (see Supporting Information Figure S5). This indicates that the bright molecules result from the interaction with the charge density redistribution around the nitrogen atoms more than a chemical interaction with nitrogen.

The electronic interaction of H_2TPP molecules with Au(111) and N-doped graphene is summarized in the diagram of Figure 4. As expected, the interaction with the substrate reduces the HOMO−LUMO gap. For an isolated molecule, the theoretical transport gap corresponds to the single-particle gap enlarged by the charging energy *U*. *Ab initio* GW calculations[36] have been used to calculate the H_2TPP HOMO−LUMO gap (including many-body effects), giving a value of 4.71 eV. The single-particle Kohn−Sham eigenvalues have also been calculated,[36] leading to a HOMO−LUMO energy gap of 1.82 eV. The charging energy *U* can thus be obtained by the difference of these two gaps, leading to *U* = 2.9 eV in the gas phase. From our STM measurements, we can estimate the charging energy by subtracting the calculated single-particle gap from the experimental values.[37] Using this procedure, we obtain charging energies $U_{Au}^{H_2TPP} \approx 0.5$ eV on Au(111) and $U_{Graphene}^{H_2TPP} \approx 1.5$ eV on graphene. The charging energy is therefore strongly reduced (by a factor of ~6) on Au(111), while it is only divided by 2 on graphene. The larger decrease of the charging energy on gold as compared to graphene can be partly understood by the fact that the density of states of graphene is lower than that of gold. Therefore, the screening effect is expected to be stronger on Au(111) than on graphene. A difference in the charge transfer between the molecules and the graphene or Au(111) substrate (expected due to the very different work functions of graphene and Au(111)) is also expected to induce a variation in the HOMO−LUMO gap of H_2TPPs. To fully understand the origin of the HOMO−LUMO gap variation of H_2TPP on Au(111) and on graphene, theoretical calculations are needed, which are beyond the scope of the present work. Concerning the interaction of porphyrins with doped graphene the experimental data can be understood as follows. H_2TPP molecules are known to be electron donors for carbon materials.[21,38] As nitrogen atoms are also donors, the two effects are competing. The charge transfer from porphyrin to graphene is reduced around the nitrogen sites, leading to a shift of the molecular states to lower energies (reducing the electron transfer from porphyrin to graphene corresponds to an n-doping of porphyrins).

CONCLUSIONS

In summary, we have studied the interaction of H_2TPP molecules with N-doped graphene. High-resolution STM imaging and spectroscopy have revealed a reduced electronic coupling of the self-organized molecules with graphene as compared to a metallic substrate. At the doping sites, we have evidenced a charge transfer from the graphene to the molecules due to the donor character of the nitrogen atoms. These findings provide a basis for a better understanding of the properties of doped graphene for the future exploitation of its chemical, catalytic, or electronic properties.

METHODS

Multilayer (~5−10) graphene samples were obtained on SiC(000$\bar{1}$) by annealing the substrates in ultrahigh vacuum (UHV) at 1320 °C for 12 min under a silicon flux of ~1 ML/min.[39,40] The nitrogen doping was performed by exposing the graphene sample to a flux of nitrogen radicals produced by a remote radio frequency plasma source.[33] Pristine and nitrogen-doped graphene samples were then transferred in air to a UHV chamber and degassed at ~800 °C for a few minutes before the measurements. The clean Au(111)/mica substrate was prepared by several cycles of Ar^+ sputtering (900 eV) followed by annealing at 330 °C under UHV. H_2TPP molecules (Aldrich) were sublimated using an effusion cell (Dr. Eberl MBE-Komponenten GmbH) under vacuum at 255 °C onto the samples at the STM stage maintained at 4.6 K. The graphene samples were then brought to room temperature for a few hours, allowing molecules to self-assemble and form a 2D island on the surface. All STM measurements were performed with a low-temperature STM apparatus (Omicron) working at 4.6 K at a pressure lower than 1×10^{-10} mbar. The d*I*/d*V* spectra were acquired using a lock-in detector at a frequency of *ca*. 670 Hz and a modulation amplitude of 35 mV. The measurements were performed with an electrochemically etched tungsten tip.

Conflict of Interest: The authors declare no competing financial interest.

Acknowledgment. V.R. thanks the Institut Universitaire de France for support.

Supporting Information Available: Additional experimental data on tip-induced hydrogen switching on H_2TPP/Au(111); voltage-dependent contrast of H_2TPP/Au(111) on N-doped graphene; atomic model of H_2TPP on N-doped graphene; energies of HOMO and LUMO states of H_2TPP on N-doped graphene. Movies showing the switch of the inner hydrogen atoms of the H_2TPP molecules on undoped (video 1) and doped (video 2) graphene, respectively. The image sizes are 10×10 nm^2 and were recorded at −1.5 V and 20 pA (video 1), 50 pA (video 2) (2 frames per second). This material is available free of charge *via* the Internet at http://pubs.acs.org.

REFERENCES AND NOTES

1. Geim, A. K.; Novoselov, K. S. The Rise of Graphene. *Nat. Mater.* **2007**, *6*, 183–191.
2. Castro Neto, A. H.; Guinea, F.; Peres, N. M. R.; Novoselov, K. S.; Geim, A. K. The Electronic Properties of Graphene. *Rev. Mod. Phys.* **2009**, *81*, 109–162.
3. Tan, X.; Chuang, H.-J.; Lin, M.-W.; Zhou, Z.; Cheng, M. M.-C. Edge Effects on the pH Response of Graphene Nanoribbon Field Effect Transistors. *J. Phys. Chem. C* **2013**, *117*, 27155–27160.
4. Yan, J.; Wang, Q.; Wei, T.; Jiang, L.; Zhang, M.; Jing, X.; Fan, Z. Template-Assisted Low Temperature Synthesis of Functionalized Graphene for Ultrahigh Volumetric Performance Supercapacitors. *ACS Nano* **2014**, *8*, 4720–4729.
5. Lee, S.-K.; Jang, H. Y.; Jang, S.; Choi, E.; Hong, B. H.; Lee, J.; Park, S.; Ahn, J.-H. All Graphene-Based Thin Film Transistors on Flexible Plastic Substrates. *Nano Lett.* **2012**, *12*, 3472–3476.
6. Rumyantsev, S.; Liu, G.; Shur, M. S.; Potyrailo, R. A.; Balandin, A. A. Selective Gas Sensing with a Single Pristine Graphene Transistor. *Nano Lett.* **2012**, *12*, 2294–2298.
7. Ko, G.; Kim, H.-Y.; Ahn, J.; Park, Y.-M.; Lee, K.-Y.; Kim, J. Graphene-Based Nitrogen Dioxide Gas Sensors. *Curr. Appl. Phys.* **2010**, *10*, 1002–1004.
8. Joshi, R. K.; Gomez, H.; Alvi, F.; Kumar, A. Graphene Films and Ribbons for Sensing of O_2, and 100 ppm of CO and NO_2 in Practical Conditions. *J. Phys. Chem. C* **2010**, *114*, 6610–6613.
9. Xue, T.; Peng, B.; Xue, M.; Zhong, X.; Chiu, C.-Y.; Yang, S.; Qu, Y.; Ruan, L.; Jiang, S.; Dubin, S.; *et al*. Integration of Molecular and Enzymatic Catalysts on Graphene for Biomimetic Generation of Antithrombotic Species. *Nat. Commun.* **2014**, *5*, 3200.
10. Kong, X.-K.; Chen, C.-L.; Chen, Q.-W. Doped Graphene for Metal-Free Catalysis. *Chem. Soc. Rev.* **2014**, *43*, 2841–2857.
11. Jiao, Y.; Zheng, Y.; Jaroniec, M.; Qiao, S. Z. Origin of the Electrocatalytic Oxygen Reduction Activity of Graphene-Based Catalysts: A Roadmap to Achieve the Best Performance. *J. Phys. Chem. C* **2014**, *136*, 4394–4403.
12. Lv, R.; Terrones, M. Towards New Graphene Materials: Doped Graphene Sheets and Nanoribbons. *Mater. Lett.* **2012**, *78*, 209–218.
13. Wang, Y.; Shao, Y.; Matson, D. W.; Li, J.; Lin, Y. Nitrogen-Doped Graphene and Its Application in Electrochemical Biosensing. *ACS Nano* **2010**, *4*, 1790–1798.
14. Qu, L.; Liu, Y.; Baek, J.-B.; Dai, L. Nitrogen-Doped Graphene as Efficient Metal-Free Electrocatalyst for Oxygen Reduction in Fuel Cells. *ACS Nano* **2010**, *4*, 1321–1326.
15. Zhang, L.; Xia, Z. Mechanisms of Oxygen Reduction Reaction on Nitrogen-Doped Graphene for Fuel Cells. *J. Phys. Chem. C* **2011**, *115*, 11170–11176.
16. Sáfar, G. d. A. M.; Martins, D. C. d. S.; DeFreitas-Silva, G.; Rebouças, J. S.; Idemori, Y. M.; Righi, A. Interactions of Porphyrins and Single Walled Carbon Nanotubes: A Fine Duet. *Synth. Met.* **2014**, *193*, 64–70.
17. Roquelet, C.; Garrot, D.; Lauret, J. S.; Voisin, C.; Alain-Rizzo, V.; Roussignol, P.; Delaire, J. A.; Deleporte, E. Quantum Efficiency of Energy Transfer in Noncovalent Carbon Nanotube/Porphyrin Compounds. *Appl. Phys. Lett.* **2010**, *97*, 141918.
18. Guo, C. X.; Lei, Y.; Li, C. M. Porphyrin Functionalized Graphene for Sensitive Electrochemical Detection of Ultratrace Explosives. *Electroanalysis* **2011**, *23*, 885–893.
19. Wu, L.; Feng, L.; Ren, J.; Qu, X. Electrochemical Detection of Dopamine Using Porphyrin-Functionalized Graphene. *Biosens. Bioelectron.* **2012**, *34*, 57–62.
20. Xu, Y.; Liu, Z.; Zhang, X.; Wang, Y.; Tian, J.; Huang, Y.; Ma, Y.; Zhang, X.; Chen, Y. A Graphene Hybrid Material Covalently Functionalized with Porphyrin: Synthesis and Optical Limiting Property. *Adv. Mater.* **2009**, *21*, 1275–1279.
21. Geng, J.; Jung, H.-T. Porphyrin Functionalized Graphene Sheets in Aqueous Suspensions: From the Preparation of Graphene Sheets to Highly Conductive Graphene Films. *J. Phys. Chem. C* **2010**, *114*, 8227–8234.
22. Auwärter, W.; Seufert, K.; Bischoff, F.; Ecija, D.; Vijayaraghavan, S.; Joshi, S.; Klappenberger, F.; Samudrala, N.; Barth, J. V. A Surface-Anchored Molecular Four-Level Conductance Switch Based on Single Proton Transfer. *Nat. Nanotechnol.* **2012**, *7*, 41–46.
23. Rojas, G.; Chen, X.; Bravo, C.; Kim, J.-H.; Kim, J.-S.; Xiao, J.; Dowben, P. A.; Gao, Y.; Zeng, X. C.; Choe, W.; *et al*. Self-Assembly and Properties of Nonmetalated Tetraphenyl-Porphyrin on Metal Substrates. *J. Phys. Chem. C* **2010**, *114*, 9408–9415.

24. Li, Z.; Smeu, M.; Ratner, M. A.; Borguet, E. Effect of Anchoring Groups on Single Molecule Charge Transport through Porphyrins. *J. Phys. Chem. C* **2013**, *117*, 14890–14898.
25. Liljeroth, P.; Repp, J.; Meyer, G. Current-Induced Hydrogen Tautomerization and Conductance Switching of Naphthalocyanine Molecules. *Science* **2007**, *317*, 1203–1206.
26. Bassiouk, M.; Alvarez-Zauco, E.; Basiuk, V. A. Self-Assemblies of Meso-Tetraphenylporphine Ligand on Surfaces of Highly Oriented Pyrolytic Graphite and Single-Walled Carbon Nanotubes: Insights from Scanning Tunneling Microscopy and Molecular Modeling. *J. Nanosci. Nanotechnol.* **2011**, *11*, 5457–5468.
27. Bussetti, G.; Campione, M.; Riva, M.; Picone, A.; Raimondo, L.; Ferraro, L.; Hogan, C.; Palummo, M.; Brambilla, A.; Finazzi, M.; *et al*. Stable Alignment of Tautomers at Room Temperature in Porphyrin 2D Layers. *Adv. Funct. Mater.* **2014**, *24*, 958–963.
28. Zhang, Y.; Brar, V. W.; Wang, F.; Girit, C.; Yayon, Y.; Panlasigui, M.; Zettl, A.; Crommie, M. F. Giant Phonon-Induced Conductance in Scanning Tunnelling Spectroscopy of Gate-Tunable Graphene. *Nat. Phys.* **2008**, *4*, 627–630.
29. Morgenstern, M. Scanning Tunneling Microscopy and Spectroscopy of Graphene on Insulating Substrates. *Phys. Status Solidi B* **2011**, *248*, 2423–2434.
30. Andrei, E. Y.; Li, G.; Du, X. Electronic Properties of Graphene: A Perspective from Scanning Tunneling Microscopy and Magnetotransport. *Rep. Prog. Phys.* **2012**, *75*, 056501.
31. Cho, J.; Smerdon, J.; Gao, L.; Süzer, Ö.; Guest, J. R.; Guisinger, N. P. Structural and Electronic Decoupling of C60 from Epitaxial Graphene on SiC. *Nano Lett.* **2012**, *12*, 3018–3024.
32. Zhao, L.; He, R.; Rim, K. T.; Schiros, T.; Kim, K. S.; Zhou, H.; Gutiérrez, C.; Chockalingam, S. P.; Arguello, C. J.; Pálová, L.; *et al*. Visualizing Individual Nitrogen Dopants in Monolayer Graphene. *Science* **2011**, *333*, 999–1003.
33. Joucken, F.; Tison, Y.; Lagoute, J.; Dumont, J.; Cabosart, D.; Zheng, B.; Repain, V.; Chacon, C.; Girard, Y.; Botello-Méndez, A. R.; *et al*. Localized State and Charge Transfer in Nitrogen-Doped Graphene. *Phys. Rev. B* **2012**, *85*, 161408.
34. Lv, R.; Li, Q.; Botello-Méndez, A. R.; Hayashi, T.; Wang, B.; Berkdemir, A.; Hao, Q.; Elías, A. L.; Cruz-Silva, R.; Gutiérrez, H. R.; *et al*. Nitrogen-Doped Graphene: Beyond Single Substitution and Enhanced Molecular Sensing. *Sci. Rep.* **2012**, *2*, 586.
35. Lambin, P.; Amara, H.; Ducastelle, F.; Henrard, L. Long-Range Interactions between Substitutional Nitrogen Dopants in Graphene: Electronic Properties Calculations. *Phys. Rev. B* **2012**, *86*, 045448.
36. Blase, X.; Attaccalite, C.; Olevano, V. First-Principles GW Calculations for Fullerenes, Porphyrins, Phtalocyanine, and Other Molecules of Interest for Organic Photovoltaic Applications. *Phys. Rev. B* **2011**, *83*, 115103.
37. Lu, X.; Grobis, M.; Khoo, K. H.; Louie, S. G.; Crommie, M. F. Charge Transfer and Screening in Individual C60 Molecules on Metal Substrates: A Scanning Tunneling Spectroscopy and Theoretical Study. *Phys. Rev. B* **2004**, *70*, 115418.
38. Geng, J.; Kong, B.-S.; Yang, S. B.; Jung, H.-T. Preparation of Graphene Relying on Porphyrin Exfoliation of Graphite. *Chem. Commun.* **2010**, *46*, 5091–5093.
39. Van Bommel, A.; Crombeen, J.; Van Tooren, A. LEED and Auger Electron Observations of the SiC(0001) Surface. *Surf. Sci.* **1975**, *48*, 463–472.
40. Varchon, F.; Mallet, P.; Magaud, L.; Veuillen, J.-Y. Rotational Disorder in Few-Layer Graphene Films on 6H-SiC (000−1): A Scanning Tunneling Microscopy Study. *Phys. Rev. B* **2008**, *77*, 165415.